

## Performance evaluation of graphene oxide coated on cotton fibers in removal of humic acid from aquatic solutions

Farnaz Tahmasebi\*, Mahmood Alimohammadi<sup>\*,\*\*,\*†</sup>, Ramin Nabizadeh\*, Mehdi Khoobi<sup>\*\*\*,\*\*\*\*</sup>, Kamaledin Karimian\*, and Ahmad Zarei<sup>\*\*\*\*\*</sup>

\*Department of Environmental Health Engineering, School of Public Health, Tehran University of Medical Sciences, Tehran, Iran

\*\*Center for Water Quality Research (CWQR), Institute for Environmental Research (IER), Tehran University of Medical Sciences, Tehran, Iran

\*\*\*Health Equity Research Center (HERC) Tehran University of Medical Sciences, Tehran, Iran

\*\*\*\*Biomaterials Group, The Institute of Pharmaceutical Sciences (TIPS), Tehran University of Medical Sciences, Tehran 1417614411, Iran

\*\*\*\*\*Department of Pharmaceutical Biomaterials and Medicinal Biomaterials Research Center, Faculty of Pharmacy, Tehran University of Medical Sciences, Tehran, Iran

\*\*\*\*\*Department of Environmental Health Engineering, Faculty of Health, Gonabad University of Medical Sciences, Gonabad, Iran

(Received 23 February 2019 • accepted 16 April 2019)

**Abstract**—We investigated the removal efficiency of humic acid from aqueous solutions by cotton coated with graphene oxide. This research has been conducted as batch on an experimental scale. A self-arrangement approach was introduced in fabrication of the cotton adsorbent coated with graphene oxide. To determine the effect of parameters, including initial concentration, pH, adsorbent dosage and contact time, central composite design (CCD) was employed in response surface method (RSM). The adsorption kinetics were determined based on different times of adsorption of humic acid. Further, the adsorption isotherms were also examined using different concentrations of humic acid. The results obtained showed that with increasing adsorbent dosage and contact time, the removal efficiency increased, while with increasing pH and initial concentration of humic acid, the removal efficiency decreased. The optimal values based on RSM method were obtained as the following: humic acid initial concentration=13.61 mg/L, pH=3.87, adsorbent dosage=0.61 g, and contact time=168.43 min. Langmuir isotherm with  $R^2=0.9987$  has been the most suitable model for explaining the adsorption process. Investigation of the adsorption kinetics indicated that humic acid adsorption follows pseudo-second-order model ( $R^2=0.9822$ ). The results indicated that the cotton adsorbent coated with graphene oxide has a good potential for removal of humic acid from aqueous solutions. Mechanical flexibility, availability, and low operational energy costs are among the advantages of this method for fabrication of this adsorbent, which can be developed and used for reducing environmental contaminants.

Keywords: Humic Acid, Adsorption, Graphene Oxide-coated Cotton, RSM

### INTRODUCTION

Natural organic compounds are a group of organic compounds originating from natural and artificial sources that exist in almost all aqueous environments. The number of organic compounds existing naturally in water resources is enormous. However, due to extreme reactivity properties, they provide the possibility of forming new organic compounds in the transfer or treatment pathway of water. In the past, the importance of natural organic compounds in drinking water was associated with aesthetic significance and development of color in water, causing complaints by consumers. However, due to the development of disinfection byproducts (DBPs)

including trihalomethanes (THMs), which are mostly carcinogenic, this issue has attracted more attention [1]. Natural organic compounds consist of hydrophobic and hydrophilic parts. The hydrophobic parts, also called humic materials, include humic acid (HA), fulvic acid (FA), and humines [2-5]. On average, humic compounds account for around 70% of soluble organic carbon content of surface waters [6]. Humic acid is one of the important humic compounds in soil. Its presence in the environment leads to formation of metal-humic acid ions and in turn transference of metals into soil. Humic acid is found in many surface and some groundwater resources. Disinfection of water resources containing humic acid by chlorine with the aim of supplying drinking water causes formation of carcinogenic disinfection byproducts including THMs. Presence of humic acid in water resources is not favorable and has been long problematic for the industry of drinking water supply. Thus, removal of humic acid from water is essential [7].

<sup>†</sup>To whom correspondence should be addressed.

E-mail: m\_alimohammadi@tums.ac.ir

Copyright by The Korean Institute of Chemical Engineers.

The most common methods for removal of humic acid from aqueous environments include coagulation [8,9], dissolved air flotation [10], filtration [11,12], ion exchange [13,14], and adsorption [15]. Among these, adsorption is the most widely used approach [16]. A wide range of adsorbents, including activated carbon [17, 18], adsorbents based on metal oxides and hydroxides [19,20], natural adsorbents [15], and nano-based adsorbents [15] were examined for this purpose.

Graphene and its derivatives enjoy favorable physiochemical characteristics owing to their unique two-dimensional structure, and as such they are of great interest across different scientific areas. Among the characteristics of graphene are desirable mechanical, electrical, thermal, and optical properties, a thickness of diameter of one or several carbon atoms, high theoretical surface area (2,630 m<sup>2</sup>/g), being harmless and environmentally friendly, low production cost, and most importantly the possibility of controlling all these characteristics through chemical functionalization [21,22]. Graphene oxide is a highly hydrophilic material, due to presence of oxygen-containing functional groups including hydroxyl, carboxyl, carbonyl, and epoxy [16,23,24].

Different methods have been applied to enhance the stability of nanoparticles on fibers. Cotton microfibers tend to alter the physical and chemical processes because they are made of poly-d-glucose chains [25].

Our aim was to examine changes in adsorption of humic acid by the adsorbent of cotton coated with graphene oxide under different conditions including contaminant concentration, contact time, adsorbent dosage, and pH to determine the best conditions for the removal of the contaminant. Eventually, isotherm and kinetic models of adsorption process were also investigated.

## MATERIALS AND METHODS

### 1. Chemicals

Hydrophilic and non-sterile cotton was purchased from a local pharmacy. Graphene oxide synthesized in the laboratory of pharmacy faculty of Tehran University of Medical Sciences, humic acid salt purchased from Acros Co., USA, sulfate acid and sodium hydroxide purchased from Merck Co.

### 2. Methods

#### 2-1. Synthesis of Graphene Oxide

Graphene oxide was prepared using graphite powder through Hummers method described in a previous study [26]. Hummers method is one of the oldest methods yet it is one of the most suitable methods for the synthesis of graphene oxide [27]. First, 5 g of graphite powder and 2.5 g of sodium nitrate were added to a 1,000

ml flask containing 120 ml of concentrated sulfuric acid in an ice bath. They were then mixed for 0.5 h at a high stirring rate. Thereafter, under these conditions, 15 g potassium permanganate was slowly added to this suspension, and was mixed for two hours. The rate of adding potassium permanganate had to be controlled carefully, such that the reaction temperature had to be kept to less than 20 °C. Next, the ice bath was removed and the mixture was exposed to room temperature for one night on a stirrer with a medium rate. As the reaction proceeded, it gradually became dough-like and its color changed into light gray. After that, under high stirring rate, 150 ml distilled water was gradually added to this dough-like mixture, when the reaction temperature was elevated immediately and brought to 98 °C. To remove the extra potassium permanganate, 50 ml oxygenated water solution (30%) was added to the slurry, whereby brown graphite oxide was obtained. For purification, the graphite oxide slurry was washed several times with HCl 5% and then with deionized water, and then filtered (or high rate centrifuge), so that the residual salt would reach natural pH. Eventually, sonication was performed for three hours. Next, several stages of centrifuge (low rate) were performed and the resulting liquid was dried in a vacuum oven (at 40 °C for 24 h). Finally, a pure powder of brown graphene oxide was obtained.

#### 2-2. Preparation of Graphene Oxide (GO) Solution

First, GO powder (1 g) was added to deionized water (1,000 ml). The suspension was then stirred by a magnetic stirrer for 30 min. Thereafter, the sonication process of the suspension was performed at 100 w for 30 min. In the next stage, the suspension was filtered through a 0.45 micron membrane for the removal of any possible GO grains. Eventually, it was kept in darkness at 4 °C until being used in the experiments. GO solution was stable across the whole duration of the experiment [21,28].

#### 2-3. Preparation of Cotton Adsorbent with Graphene Oxide Coating

First, 0.5 g of cotton was washed with double distilled water and then exposed to 80 °C in an oven for the entire night, in order to be dried completely. The dried cotton was then immersed in 30 ml graphene oxide suspension 1 g/L. Thereafter, the mixture was heated in the oven at 90 °C for 4 h. Eventually, the obtained cotton coated with graphene was separated from the solution and placed inside the oven at 100 °C throughout the night to be dried completely.

After several replications, the cotton fibers smeared with graphene oxide were washed with deionized water and then placed inside the oven at 100 °C for 24 h. By calculating the difference of the final weight of the cotton fibers modified with graphene oxide and its initial weight, one can obtain the level of graphene oxide. The coated cotton fibers were kept inside suitable containers for fur-

**Table 1. Experimental factors and levels in the central composite design for the HA adsorption**

Factors	Levels				
	Low (-1)	Central (0)	High (+1)	- $\alpha$	+ $\alpha$
X <sub>1</sub> : HA concentration (mg/L)	10	30	50	20	40
X <sub>2</sub> : Adsorbent dosage (gr)	0.2	0.45	0.7	0.325	0.575
X <sub>3</sub> : Time (min)	15	97.5	180	56.25	138.75
X <sub>4</sub> : pH	3	6	9	4.5	7.5

ther experiments [29]. To detect the superficial characteristics of the adsorbent, FE-SEM analysis (SIGMA VP-500) was performed. Also, the presence of graphene oxide and cellulose was observed using x-ray diffraction device (XRD). For identification of the functional groups of the adsorbent surface, FTIR analysis was utilized.

### 3. Experimental Design

For design of the experiments, response surface method (RSM) was chosen, the target of which is optimization of the desired response [30]. From different designs of RSM, central composite design (CCD) was selected for modeling and optimizing processes [31-33]. In the first stage, the design of the number of factors was

determined. In this study, the final range of variables was determined based on previous studies on the removal of humic acid by adsorption process (Table 1). Generally, the number of test procedures in the software is calculated according to the formula  $N = 2^K + 2K + C$ , where  $K$  is the number of factors involved and  $C$  is the number of repetitions of the test steps. Finally, 38 runs were determined by R software (3.1.3). The data of the CCD design method were used to determine the equivalence of quadratic polynomial regression equations as Eq. (1):

$$Y = \beta_0 + \sum_{j=1}^K \beta_j X_j + \sum_{j=1}^K \beta_{jj} X_j^2 + \sum_{j=1}^K \sum_{i=1}^K \beta_{ij} X_j X_i + \varepsilon \quad (1)$$

In Table 2, the experimental conditions and the results of the removal of humic acid by cotton-coated graphene oxide are presented according to the design of the test.

### 4. Adsorption Experiments

#### 4-1. Batch Adsorption Experiments

All of the experiments were performed in a batch mode. After preparing stock solution of humic acid, the concentrations of interest were prepared from the stock solution. For adjustment of pH of each of the concentrations of interest, sulfuric acid and sodium hydroxide 0.1 N were used. After pH adjustment, the predetermined adsorbent dosage was weighed according to the determined runs and was added to the humic acid containing solution. The samples were placed on a shaker under the conditions of 1,150 rpm, temperature of 25 °C, and the contact time of interest for suitable mixing. Thereafter, the samples were centrifuged at 4,000 rpm for 10 min, and then passed through a filter with pore diameter of 0.45 micrometer. Finally, the residual concentration of humic acid was measured.

#### 4-2. Isotherm and Kinetic Studies

To express the behavior of humic acid adsorption on GO-cotton, isotherm experiments were carried out under optimized conditions and the obtained data were matched to Langmuir, Freundlich and Temkin models (Table 3). To evaluate the transfer rate of humic acid on graphene oxide coated cotton fibers, kinetic experiments were carried out under optimized conditions and the experimental data were matched to first-order and pseudo-second-order models (Table 3).

## RESULTS AND DISCUSSION

### 1. Characterization of the Synthesized Adsorbent

XRD analysis related to graphene oxide and the graphene oxide-

**Table 2. CCD experimental design for HA removal by GO-cotton**

Run order	Std. order	X <sub>1</sub> (mg/L)	X <sub>2</sub> (g)	X <sub>3</sub> (min)	X <sub>4</sub>	Removal (%)
1	2	40	0.325	56.25	4.5	40.23
2	8	40	0.575	138.75	4.5	71.65
3	6	40	0.325	138.75	4.5	46.49
4	18	30	0.45	97.5	6	50.19
5	3	20	0.575	56.25	4.5	75.08
6	22	30	0.45	97.5	6	61.36
7	13	20	0.325	138.75	7.5	47.52
8	12	40	0.575	56.25	7.5	43.39
9	17	30	0.45	97.5	6	49.64
10	16	40	0.575	138.75	7.5	48.37
11	10	40	0.325	56.25	7.5	36.61
12	11	20	0.575	56.25	7.5	48.39
13	15	20	0.575	138.75	7.5	55.71
14	5	20	0.325	138.75	4.5	53.75
15	21	30	0.45	97.5	6	51.61
16	14	40	0.325	138.75	7.5	41.38
17	4	40	0.575	56.25	4.5	67.46
18	1	20	0.325	56.25	4.5	65.43
19	19	30	0.45	97.5	6	50.67
20	20	30	0.45	97.5	6	49.83
21	9	20	0.325	56.25	7.5	41.28
22	7	20	0.575	138.75	4.5	79.67
1	8	30	0.45	97.5	9	33.61
2	10	30	0.45	97.5	6	51.47
3	5	30	0.45	15	6	54/83
4	11	30	0.45	97.5	6	50.67
5	2	50	0.45	97.5	6	53.17
6	15	30	0.45	97.5	6	50.29
7	16	30	0.45	97.5	6	49.91
8	12	30	0.45	97.5	6	51.11
9	7	30	0.45	97.5	3	72.41
10	13	30	0.45	97.5	6	49.66
11	1	10	0.45	97.5	6	67.39
12	6	30	0.45	180	6	68.65
13	9	30	0.45	97.5	6	50.33
14	4	30	0.7	97.5	6	70.92
15	14	30	0.45	97.5	6	49.73
16	3	30	0.2	97.5	6	45.4

**Table 3. Equations of isotherm and adsorption kinetics [34-36]**

Model	Equation
Langmuir isotherm	$q_e = \frac{Q_m K_L C_e}{1 + K_L C_e}$
Freundlich isotherm	$q_e = K_f C_e^{\frac{1}{n}}$
Temkin isotherm	$q_e = A_T + B_T \log C_e$
Pseudo-first-order kinetic	$\frac{dq_t}{dt} = K_1 (q_e - q_t)$
Pseudo-second-order kinetic	$\frac{dq_t}{dt} = K_2 (q_e - q_t)^2$

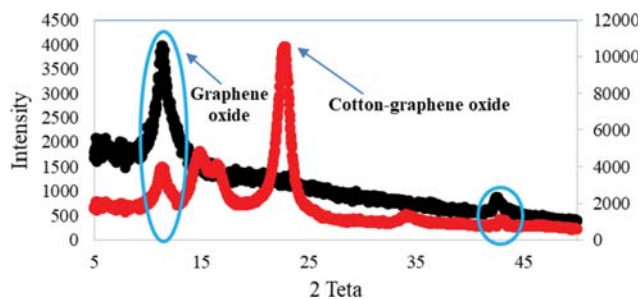


Fig. 1. XRD pattern of graphene oxide and cotton-graphene oxide.

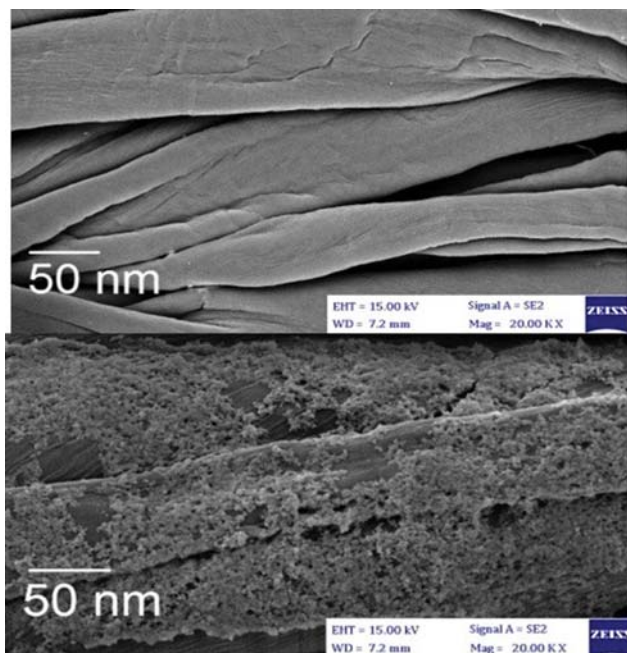


Fig. 2. FE-SEM images of cotton and cotton-graphene oxide.

cotton composite is represented in Fig. 1. The peaks at 14.83, 16.48, 22.66, and 34.27  $^{\circ}$ , according to the standard presented in JCPDS file no 3-0226, belong to cellulose, suggesting the presence of cotton in the structure of the studied composite. The peaks developed at 12.15 and 42.7  $^{\circ}$  also represent the presence of graphene oxide [37].

To identify the superficial characteristics of graphene oxide as well as the synthesized composite, FE-SEM analysis was employed (Fig. 2). As can be observed, the surface of cotton is observed at cylindrical and interwoven, where no protrusion lies on it. Based on this analysis, the diameter of cotton was obtained as 86 nm. After stabilization of graphene oxide on cotton, the composite surface became irregular, rougher and, wrinkled, which is very suitable for transferring the contaminant to the adsorbent surface. Indeed, it causes improved mass transfer from the adsorbate to the adsorbent. The diameter range of the synthesized composite was between 22-50 nm.

For more accurate investigation of the stabilization of graphene oxide, the functional groups within the cotton structure were examined through FTIR analysis within 400-4,000/cm. The peak devel-

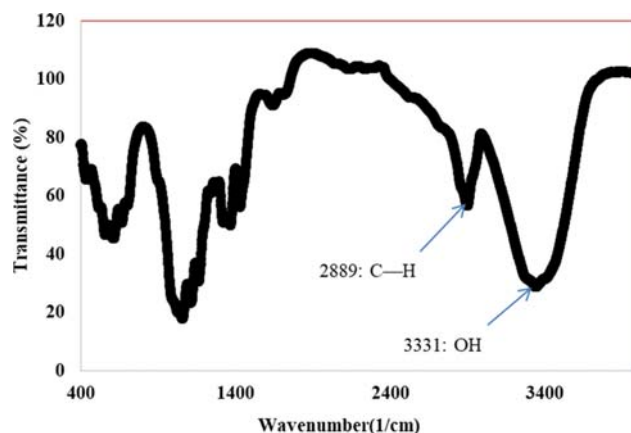


Fig. 3. FTIR spectrum of cotton-graphene oxide adsorbent.

oped at 3,331  $\text{cm}^{-1}$  represents vibration band associated with O-H bond, and the peak at 2,889  $\text{cm}^{-1}$  shows the vibrations resulting from C-H. The bands associated with bending vibrations of O-H,  $\text{CH}_2$ , and CH bonds can also be identified by the peaks of 1,648, 1,428, and 1,315  $\text{cm}^{-1}$ . All of the mentioned peaks can be observed within the graphene oxide structure (Fig. 3). The peaks developed within 900-1,400  $\text{cm}^{-1}$  are a strong evidence regarding presence of cellulose within the structure of the synthesized composite. These results are in accordance with similar cases performed by XRD analysis [37]. Previous studies on synthesis of cotton by Sahito et al. showed that in FTIR diagram, a peak at 875  $\text{cm}^{-1}$  related to C-C vibration should be seen within the cotton structure, which was not observed in the present study. This is because this bond is also presented in GO, and cannot confirm cotton [38].

### 3-2. Effect of Initial Concentration of Humic Acid on the Adsorption Process

To examine the effect of initial concentration of humic acid on the removal efficiency, humic acid solutions with concentrations of 10-50 mg/L were prepared. Fig. 4(a) shows that by increasing the concentration of humic acid, the removal efficiency decreases. Thus, at lower concentrations of humic acid, adsorption occurs in the entrance areas of the pores or in areas close to the input mouth of the pores. Due to the short pathway of diffusion in this state and presence of adequate space for adsorption of a certain amount of contaminants, adsorption occurs faster and more rapidly. However, at higher concentrations, these regions are saturated quickly and further adsorption requires diffusion in deeper areas of the pores through diffusion or traversing a relatively long path, resulting in diminished adsorption efficiency [39].

### 3. Effect of Adsorbent Dosage on the Adsorption Process

To investigate the effect of the amount of adsorbent on the removal efficiency, the adsorbent dosages were examined within 0.2-0.7 g. This study showed that increasing the level of adsorbent has a direct effect on the removal efficiency of humic acid (Fig. 4(b)). Increasing the extent of active and effective surface area of the adsorbent results in increased adsorption efficiency. Although with increasing the adsorbent level the removal efficiency increases, as some of the active points present on the adsorbent surface remain unsaturated, and thus the adsorbent is not used by its full capac-

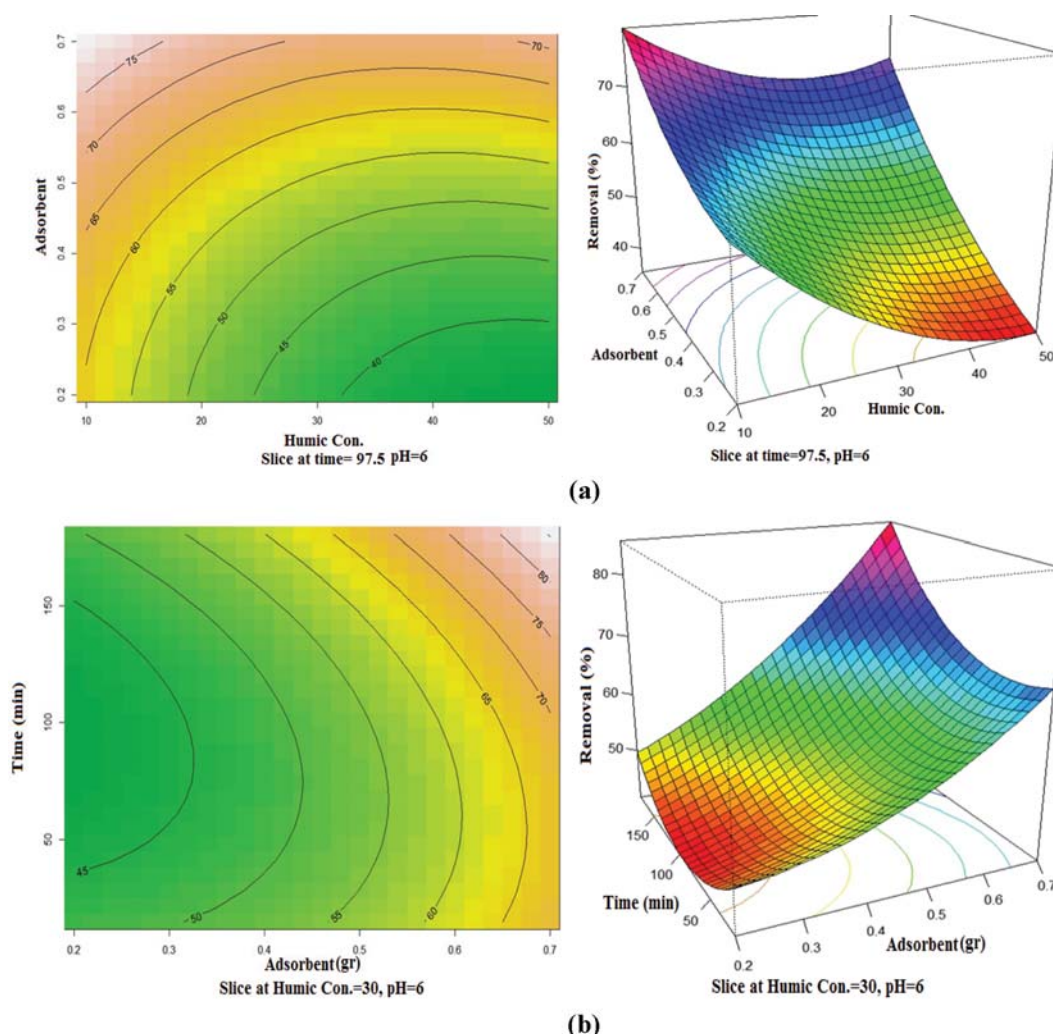


Fig. 4. Contour and 3D response surface plots for HA removal. The effect of (a) initial HA concentration and GO-Cotton mass, (b) GO-Cotton mass and time, (c) time and pH and (d) pH and GO-Cotton mass.

ity, the extent of adsorption per unit of the adsorbent mass diminishes [17,40].

#### 4. Effect of Contact Time on the Adsorption Process

To examine the effect of contact time on the adsorption process, adsorption experiments were performed within the time range of 15–180 min. Based on the results, the removal efficiency increases with prolongation of contact time (Fig. 4(c)), and after about 170 min, it has reached equilibrium. The experiments showed that the amount of adsorbed humic acid gradually increased; with increasing contact time, the rate of adsorption was initially rapid, and then gradually decreased over time to reach equilibrium [16,17,41].

#### 5. Effect of Initial pH of the Solution on the Adsorption Process

To investigate the effect of pH on the removal efficiency, experiments were performed within the pH range of 3–9. pH is the most important variable which affects the zeta potential. Therefore, the pH of the solution affects both the surface charge of the adsorbent and the humic acid charge, and these conditions control the humic acid adsorption. Note that Zeta potential, regardless of pH value, is a nearly meaningless concept. The pH value at which the number

of the positively and negatively charges on an adsorbent surface are equal is expressed as the point of zero charge value (pHpzc). The values of points of zero charge (pHpzc) for all the adsorbents can be estimated following an acid-base titration technique proposed by Li et al. [42]. The pHpzc value of pHpzc was estimated to be 3.7 for the GO-cotton. This is somewhat near to the results of a previous work [43]. At  $\text{pH} < \text{pHpzc}$ , the surface charge of graphene oxide will be positive due to the adsorption of  $\text{H}^+$  ions, while negatively charged at pH above pHpzc due to the adsorption of  $\text{OH}^-$  ions. Humic acid structure has a mixture of compounds with weakly acidic functional groups, including phenolic and carboxylic groups. Thereby, the main mechanisms involved in the uptake of humic acid from an aqueous media by adsorption onto sorbents could be due to one or a combination of some factors including ionic attraction, physical adsorption and intra-particle diffusion [3,4,44,45]. The charge of humic acid is negatively affected by the presence of carboxylic and phenol groups; therefore, adsorption of humic acid on the adsorbent occurs at acidic pH (Fig. 4(d)). In acidic pHs, humic acid has a high solubility, and this has effects on its adsorption. At high pH values, the surface charge of graphene oxide will

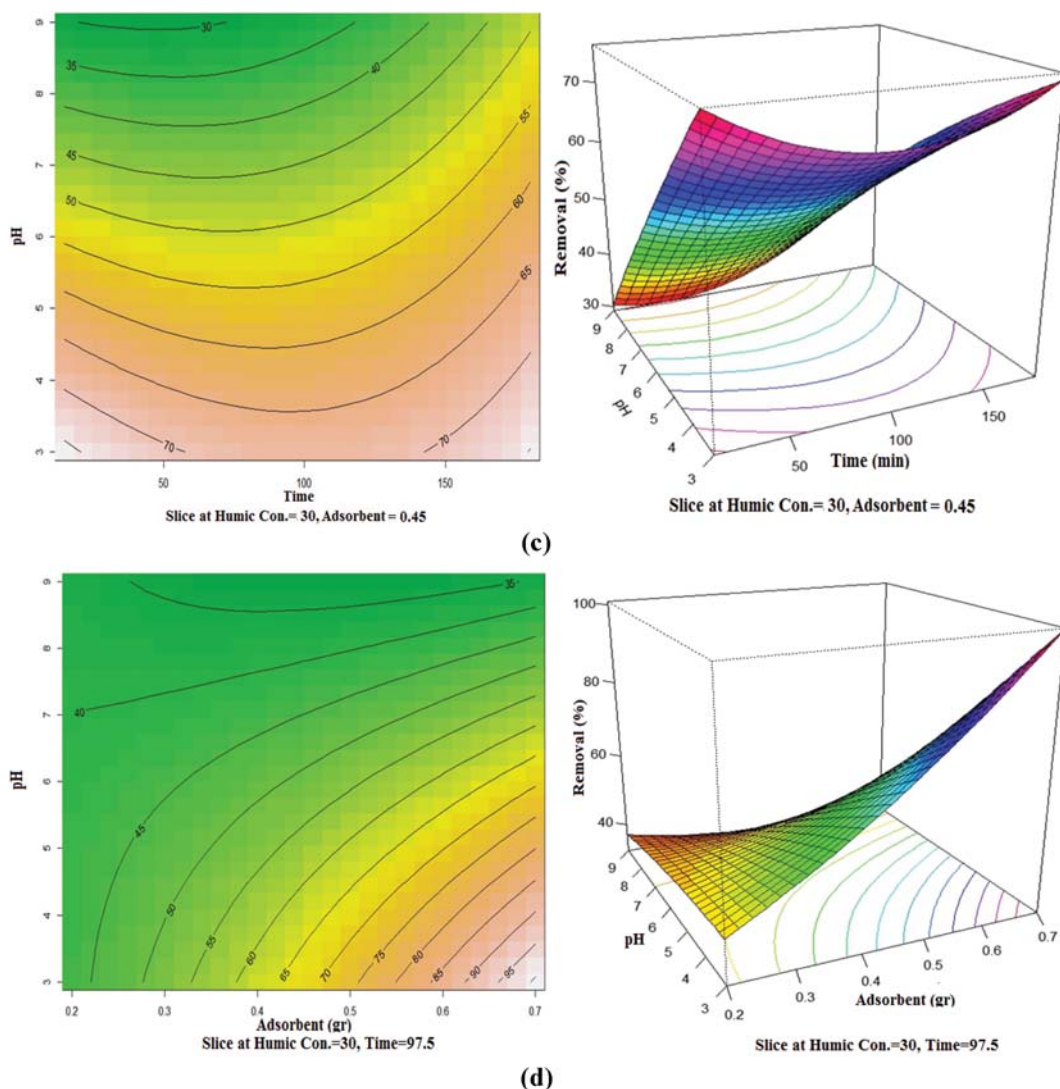


Fig. 4. Continued.

change. Further, carboxylic and phenolic groups of humic acid also begin to dissociate. Therefore, its adsorption on the graphene oxide surface will be difficult. With increasing the solution acidity, the adsorption efficiency increases due to the electrostatic adsorption forces between the adsorbent and humic acid. At alkaline pH, due to repulsive electrostatic force occurring, it is probable that with increasing the pH, the spherical shape of humic acid molecules becomes linear and this decreases the humic acid adsorption in higher pHs [7,40,41].

#### 6. Desorption Studies

One of the important characteristics of an adsorbent is its ability to be regenerated. A desorption study provides good information to evaluate the nature of adsorption process and to reuse the used adsorbent. The most common desorbing chemicals used to desorb the adsorbates are NaOH, HCl, HNO<sub>3</sub>, EDTA, CaCl<sub>2</sub>, and organic solvents including methanol and ethanol [46]. Regeneration of GO-cotton and desorption of humic acid was studied by eluting the HA using HCl as eluent. For desorption tests, humic acid was initially adsorbed by GO-cotton. After that, 0.1 M HCl

was used for desorption study. The removal efficiency of the regenerated GO-cotton was investigated in the three cycles of adsorption-desorption. The findings of desorption tests revealed that 86%,

**Table 4. Isotherm models and the parameters of fitted models for HA adsorption onto GO-Cotton**

Isotherm	Parameters	
Langmuir	$K_L$	15.84
	$q_m$ (mg/g)	57.59
	$R^2$	0.9978
	$R_L$	0.0012-0.012
Freundlich	$K_F$	38.18
	$n$	6.21
	$R^2$	0.9884
Temkin	$K_t$	13769.2
	$B$	4.63
	$R^2$	0.9468

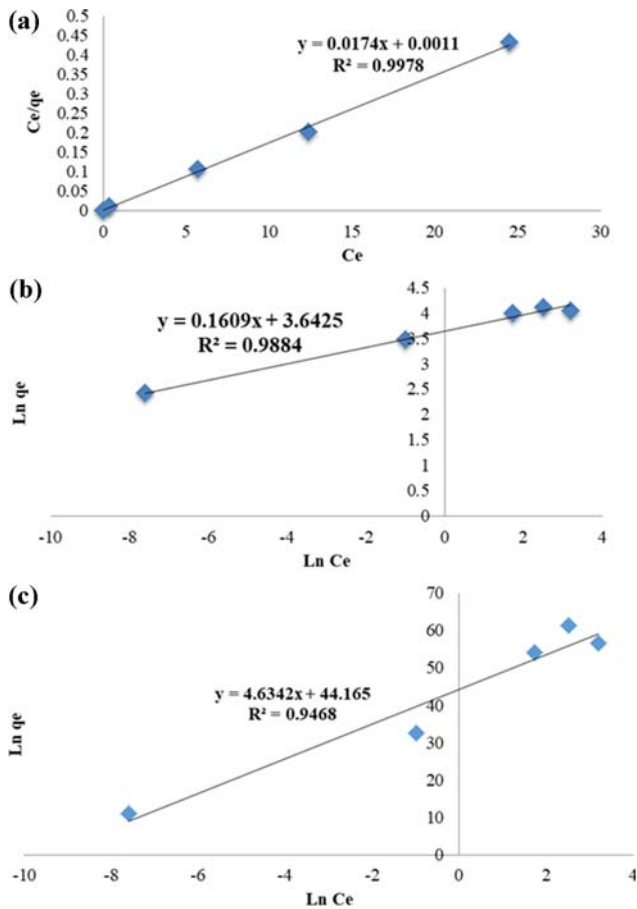


Fig. 5. Adsorption isotherms of humic acid (a) Langmuir, (b) Freundlich and (c) Temkin.

68% and 48% of humic acid removed from GO-cotton at optimum operating conditions, respectively, in first, second and third cycles. As higher concentration of HCl, higher desorption of humic acid occurred.

**7. Adsorption Isotherm**

The adsorption isotherm is an important parameter in designing adsorption systems and well represents the relationship between the concentration of adsorbate and adsorption capacity of the adsorbent [47,48]. Table 4 lists the fitted isotherm models, their linear forms, and the values of parameters obtained by fitting the experimental data with the models and shown in Fig. 5(a)-(c). As seen, the value of R<sup>2</sup> is higher for Langmuir model than the other models. The adsorption theory of Langmuir model is based on the monolayer surface adsorption on the ideal solid with definite localized sites that are energetically identical [49,50]. As seen in Table 4, the maximum monolayer adsorption capacity of GO-Cotton for HA was 57.59 mg/g in the present work.

**8. Adsorption Kinetics**

Adsorption kinetics is important for designing adsorption systems and determining the retention time of the adsorbent in the adsorption process. Adsorption kinetics depends on the physiochemical properties of the adsorbent. Table 5 shows the fitted experimental data with the pseudo-first order and pseudo-second order kinetic models. As seen, pseudo-second-order kinetic model with

Table 5. Constants obtained from kinetic models for HA adsorption onto GO-Cotton

Kinetic models	Parameters	
Pseudo-first-order	K <sub>1</sub>	0.02854
	q <sub>e</sub> (cal) (mg/g)	63.8304
	R <sup>2</sup>	0.9742
Pseudo-second-order	K <sub>1</sub>	0.000300405
	q <sub>e</sub>	82.22
	R <sup>2</sup>	0.9822

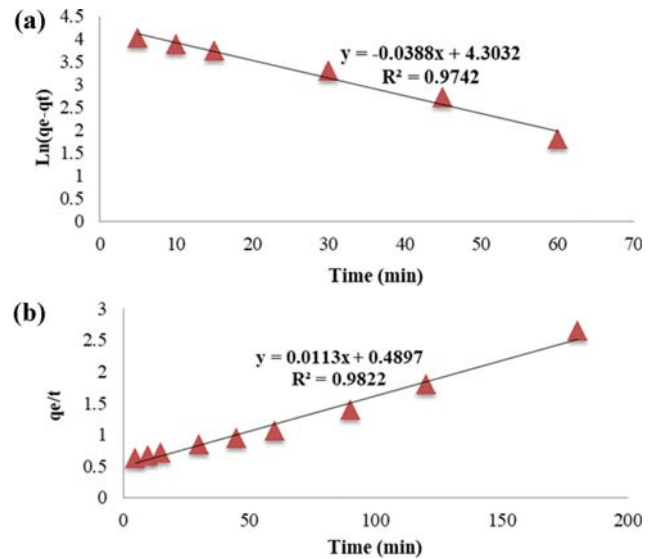


Fig. 6. The diagram of humic acid adsorption kinetics (a) pseudo-first-order, (b) pseudo-second order.

higher R<sup>2</sup> values showed better compliance with the experimental data, suggesting the adsorption to be controlled by chemisorption [49,51].

Table 6. Estimated coefficients of the fitted polynomial model for HA adsorption onto GO-Cotton

	Estimate	S td. error	t Value	Pr(> t )
(Intercept)	51.1764	1.0502	48.7284	< 2.2e-16***
X <sub>1</sub>	-8.3075	1.6043	-5.1784	3.000e-05***
X <sub>2</sub>	14.0058	1.6043	8.7304	9.280e-09***
X <sub>3</sub>	4.5258	1.6043	2.8211	0.009688**
X <sub>4</sub>	-17.8925	1.6043	-11.1531	9.386e-11***
X <sub>1</sub> : X <sub>2</sub>	3.8225	3.9296	0.9727	0.340804
X <sub>1</sub> : X <sub>3</sub>	3.4325	3.9296	0.8735	0.391424
X <sub>1</sub> : X <sub>4</sub>	6.2375	3.9296	1.5873	0.126099
X <sub>2</sub> : X <sub>3</sub>	3.8725	3.9296	0.9855	0.334652
X <sub>2</sub> : X <sub>4</sub>	-14.7225	3.9296	-3.7465	0.001053**
X <sub>3</sub> : X <sub>4</sub>	4.9875	3.9296	1.2692	0.217062
X <sub>1</sub> <sup>2</sup>	6.1723	2.7454	2.2482	0.034443*
X <sub>2</sub> <sup>2</sup>	4.0523	2.7454	1.4760	0.153492
X <sub>3</sub> <sup>2</sup>	7.6323	2.7454	2.7800	0.010646*
X <sub>4</sub> <sup>2</sup>	-1.0977	2.7454	-0.3998	0.692974

**Table 7. Analysis of variance (ANOVA) for the fitted polynomial model for HA adsorption onto GO-Cotton**

Model formula		Df	Sum Sq	Mean Sq	F value
First-order response	4	3634.8	908.70	58.8462	9.519e-12
Second-order response	6	321.9	53.65		3.4745
Pure quadratic response	4	242.7	60.68		3.9298
Residuals	23	355.2	15.44		
Lack of fit	10	238.0	23.80		2.6415
Pure error	13	117.1	9.01		

Notes: Multiple R-squared: 0.922, Adjusted R-squared: 0.8746 F-statistic: 19.43 on 14 and 23 DF, p-value: 1.763e-09

## 9. Model Fitting and Statistical Analysis

Table 6 summarizes the analysis of variance (ANOVA) of the experimental data presented in Table 2. The results of this analysis, which is a full quadratic analysis, show that the three variables  $X_1$ ,  $X_2$  and  $X_3$  with intercept at the level of 0.001 and the  $X_3$  variable are also affected at 0.05 on the efficiency of the removal. Among interactions, only the interactions between pH and adsorbent dose ( $X_2$ ;  $X_4$ ) are significant at 0.01 levels. However, the results of this analysis indicate that the second exponent of the variable  $X_1$ , the concentration of humic acid, as well as the second exponent of the  $X_3$  variable or contact time, also affect the level of 0.05, but the second exponent of other variables, as well as the interaction between them, is ineffective. By applying RSM method and according to Table 6, Eq. (2) which represents an experimental relationship between the variables of the experiment and efficiency percentage as coded, has been presented:

$$\begin{aligned}
 Y = & 51.1764 - 8.3075X_1 + 14.0058X_2 + 4.5258X_3 - 17.8925X_4 \\
 & + 3.8225X_1 \times X_2 + 3.4325X_1 \times X_3 + 6.2375X_1 \times X_4 \\
 & + 3.8725X_2 \times X_3 - 14.7225X_2 \times X_4 + 4.9875X_3 \times X_4 \\
 & + 6.1723X_1^2 + 4.0523X_2^2 + 7.6323X_3^2 - 1.0977X_4^2
 \end{aligned} \quad (2)$$

where, Y represents the removal efficiency,  $X_1$  is the humic acid concentration,  $X_2$  is the amount of adsorbent used,  $X_3$  is the contact time, and  $X_4$  is pH value.

As shown in Table 7,  $R^2$  is also 0.992, and the difference with the adjusted  $R^2$  is less than 0.2. The lack of fit of this model is 0.051, which is more than 0.05, suggesting that removal of humic acid by graphene oxide adsorbent coated with cotton fiber can be defined by this model.

## CONCLUSIONS

Graphene oxide with cotton fiber coating adsorbent was used for removal of humic acid from aqueous solutions. Surface response method was used based on CCD design for evaluating the effect of independent variables, including initial concentration of humic acid, amount of adsorbent used, contact time, and pH on response performance (removal efficiency of humic acid). The maximum removal efficiency was obtained at humic acid initial concentration of 13.6 mg/L, contact time of 168.43 min, pH of 3.8, and adsorbent value of 0.61. For increasing the stability and further distribution of graphene oxide nanoparticles, cotton coating was employed, and its ability in absorbing humic acid was examined. Mechanical flexibility, availability, and low operational energy costs

are among the advantages of this method for fabrication of this adsorbent, which can be developed and utilized for mitigating environmental contaminants. Overall, the results obtained from this study indicated that GO-Cotton enjoys a good potential for the removal of humic acid from aqueous solutions.

## ACKNOWLEDGEMENTS

This research was supported by Water Quality Research (CWQR), Institute for Environmental Research (IER), Tehran University of Medical Sciences, Grant (Project Number 95-02-46-32200).

## CONFLICT OF INTEREST

The authors of this article declare that they have no conflict of interests.

## REFERENCES

1. R. Saeedi, K. Naddafi, R. Nabizadeh, A. Mesdaghinia, S. Nasser, M. Alimohammadi and S. Nazmara, *Environ. Eng. Sci.*, **29**, 93 (2012).
2. S. Song, S. Huang, R. Zhang, Z. Chen, T. Wen, S. Wang, T. Hayat, A. Alsaedi and X. Wang, *Chem. Eng. J.*, **325**, 576 (2017).
3. S. Huang, S. Song, R. Zhang, T. Wen, X. Wang, S. Yu, W. Song, T. Hayat, A. Alsaedi and X. Wang, *ACS Sustainable Chem. Eng.*, **5**, 11268 (2017).
4. T. Wen, J. Wang, S. Yu, Z. Chen, T. Hayat and X. Wang, *ACS Sustainable Chem. Eng.*, **5**, 4371 (2017).
5. T. Wen, Q. Fan, X. Tan, Y. Chen, C. Chen, A. Xu and X. Wang, *Polym. Chem.*, **7**, 785 (2016).
6. A. De la Rubia, M. Rodríguez, V.M. León and D. Prats, *Water Res.*, **42**, 714 (2008).
7. T. Hartono, S. Wang, Q. Ma and Z. Zhu, *J. Colloid Interface Sci.*, **333**, 114 (2009).
8. M. Askari, M. Alimohammadi, M. H. Dehghani, M. M. Emamjomeh and S. Nazmara, *J. Adv. Environ. Health Res.*, **2** (2014).
9. M. Alimohammadi, M. Askari, M. Dehghani, A. Dalvand, R. Saeedi, K. Yetilmezsoy, B. Heibati and G. McKay, *Int. J. Environ. Sci. Technol.*, **14**, 2125 (2017).
10. Y. Shutova, B. L. Karna, A. C. Hambly, B. Lau, R. K. Henderson and P. Le-Clech, *Desalination*, **383**, 12 (2016).
11. J. J. Song, Y. Huang, S.-W. Nam, M. Yu, J. Heo, N. Her, J. R. Flora and Y. Yoon, *Sep. Purif. Technol.*, **144**, 162 (2015).
12. M. Kumar, Z. Gholamvand, A. Morrissey, K. Nolan, M. Ulbricht

- and J. Lawler, *J. Membr. Sci.*, **506**, 38 (2016).
13. Z. Ren and N. Graham, *Environ. Eng. Sci.*, **32**, 175 (2015).
  14. C. Shuang, M. Wang, Q. Zhou, W. Zhou and A. Li, *Water Res.*, **47**, 6406 (2013).
  15. A. Bhatnagar and M. Sillanpää, *Chemosphere*, **166**, 497 (2017).
  16. N. Cai, D. Peak and P. Larese-Casanova, *Chem. Eng. J.*, **273**, 568 (2015).
  17. N. T. Tavengwa, L. Chimuka and L. Tichagwa, *Desalination Water Treatment*, **57**, 16843 (2016).
  18. S. Velten, D. R. Knappe, J. Traber, H.-P. Kaiser, U. Von Gunten, M. Boller and S. Meylan, *Water Res.*, **45**, 3951 (2011).
  19. C. Ding and C. Shang, *Water Res.*, **44**, 3651 (2010).
  20. Y. Zhang, M. Li, S. Wu and Q. Zhang, *Desalination Water Treatment* **57**, 1940 (2016).
  21. X. Wang, S. Yu, J. Jin, H. Wang, N. S. Alharbi, A. Alsaedi, T. Hayat and X. Wang, *Sci. Bulletin*, **61**, 1583 (2016).
  22. X. Wang, S. Yu, Z. Chen, Y. Zhao, J. Jin and X. Wang, *Sci. China Chem.*, **60**, 1149 (2017).
  23. Y. Zhu, S. Murali, W. Cai, X. Li, J. W. Suk, J. R. Potts and R. S. Ruoff, *Adv. Mater.*, **22**, 3906 (2010).
  24. G. Zhao, J. Li, X. Ren, C. Chen and X. Wang, *Environ. Sci. Technol.*, **45**, 10454 (2011).
  25. I. Montesinos, A. Sfakianaki, M. Gallego and C. D. Stalikas, *J. Sep. Sci.*, **38**, 836 (2015).
  26. L. Shahriary and A. A. Athawale, *Int. J. Renew. Energy Environ. Eng.*, **2**, 58 (2014).
  27. W. S. Hummers Jr. and R. E. Offeman, *J. Am. Chem. Soc.*, **80**, 1339 (1958).
  28. L. Duan, R. Hao, Z. Xu, X. He, A. S. Adeleye and Y. Li, *Chemosphere*, **168**, 1051 (2017).
  29. S. S. Khaloo, M. Ahmadi Marzaleh, M. Kavousian and S. Bahramzadeh Gendeshmin, *Sep. Sci. Technol.*, **51**, 1 (2016).
  30. A. Dehghan, A. Zarei, J. Jaafari, M. Shams and A. M. Khaneghah, *Chemosphere*, **217**, 250 (2019).
  31. J. M. Aquino, R. C. Rocha-Filho, N. Bocchi and S. R. Biaggio, *J. Environ. Chem. Eng.*, **1**, 954 (2013).
  32. R. Rezaee, A. Maleki, A. Jafari, S. Mazloomi, Y. Zandsalimi and A. H. Mahvi, *J. Environ. Health Sci. Eng.*, **12**, 67 (2014).
  33. J. Wu, H. Zhang, N. Oturan, Y. Wang, L. Chen and M. A. Oturan, *Chemosphere*, **87**, 614 (2012).
  34. S. Mazloomi, M. Yousefi, H. Nourmoradi and M. Shams, *J. Environ. Health Sci. Eng.*, **1** (2019).
  35. M. H. Dehghani, S. Kamalian, M. Shayeghi, M. Yousefi, Z. Heidarinejad, S. Agarwal and V. K. Gupta, *Microchem. J.*, **145**, 486 (2019).
  36. M. H. Dehghani, S. Tajik, A. Panahi, M. Khezri, A. Zarei, Z. Heidarinejad and M. Yousefi, *MethodsX*, **5**, 1148 (2018).
  37. N. D. Tissera, R. N. Wijesena, J. R. Perera, K. N. de Silva and G. A. Amaraturunge, *Appl. Surf. Sci.*, **324**, 455 (2015).
  38. I. A. Sahito, K. C. Sun, A. A. Arbab, M. B. Qadir and S. H. Jeong, *Carbohydr. Polym.*, **130**, 299 (2015).
  39. V. Oskoei, M. Dehghani, S. Nazmara, B. Heibati, M. Asif, I. Tyagi, S. Agarwal and V. K. Gupta, *J. Mol. Liq.*, **213**, 374 (2016).
  40. W. Song, D. Shao, S. Lu and X. Wang, *Sci. China Chem.*, **57**, 1291 (2014).
  41. Z. Liu, X. Wang, Z. Luo, M. Huo, J. Wu, H. Huo and W. Yang, *PLoS One*, **10**, e0143819 (2015).
  42. J. Hur, J. Shin, J. Yoo and Y.-S. Seo, *The Scientific World J.*, **2015**, (2015).
  43. P. Nuengmacha, R. Mahachai and S. Chanthai, *Oriental J. Chem.*, **30**, 1463 (2014).
  44. M. H. Dehghani, A. Mesdaghinia, R. Nabizadeh, M. Alimohammadi, M. Afsharnia and G. McKay, *Chem. Eng. Res. Design*, **140**, 102 (2014).
  45. L. Tan, X. Tan, M. Fang, X. Wang, J. Wang, J. Xing, Y. Ai and X. Wang, *Environ. Pollution*, **246**, 999 (2019).
  46. M. Zulfikar, E. Novita, R. Hertadi and S. Djajanti, *Int. J. Environ. Sci. Technol.*, **10**, 1357 (2013).
  47. K. Foo and B. Hameed, *Chem. Eng. J.*, **156**, 2 (2010).
  48. M. Qasemi, A. Zarei, M. Afsharnia, R. Salehi, M. Allahdadi and M. Farhang, *Data in Brief*, **20**, 1115 (2018).
  49. M. Shams, M. H. Dehghani, R. Nabizadeh, A. Mesdaghinia, M. Alimohammadi and A. A. Najafpoor, *J. Mol. Liq.*, **224**, 151 (2016).
  50. M. Qasemi, M. Afsharnia, A. Zarei, A. A. Najafpoor, S. Salari and M. Shams, *Data in Brief*, **18**, 620 (2018).
  51. R. Khosravi, H. Eslami, A. Zarei, M. Heidari, A. N. Baghani, N. Safavi, A. Mokammel, M. Fazlzadeh and S. Adhami, *Desalination Water Treatment*, **116**, 119 (2018).